Supporting Information for

Lightly Fe-doped (NiS_2/MoS_2)/Carbon Nanotube Hybrid Electrocatalyst Film with Laser-Drilled Micropores for Stabilized Overall Water Splitting and pH-Universal Hydrogen Evolution Reaction

Chenyu Li, [a] Mingda Liu, [a] Hanyuan Ding, [a] Liqiong He, [a] Enze Wang, [a] Bolun Wang, [a] Shoushan Fan [b] and Kai Liu*,[a]

[a] State Key Laboratory of New Ceramics and Fine Processing, School of Materials Science and Engineering, Tsinghua University, Beijing 100084, P. R. China.

[b] Department of Physics and Tsinghua-Foxconn Nanotechnology Research Center, Tsinghua University, Beijing 100084, P. R. China.

* Corresponding Author. E-mail: liuk@tsinghua.edu.cn; Tel: +86-10-62799182.

Experimental Section

Preparation of CNT film

CNT films were derived from a super-aligned carbon nanotube (SACNT) array, which was synthesized in a low pressure chemical vapor deposition system, as reported in our previous work.[S1] In the SACNT array, CNTs are much denser and aligned much better than those in ordinary arrays, and have very clean surface and good electrical conductivity with few defects.[S2] To prepare our CNT film, 20 mg CNTs were removed out of the SACNT array into 250 ml ethanol and dispersed under high-power probe ultrasonication (SCIENTZ-950E) for 5 minutes. Then, a CNT film was fabricated by suction filtration from the above mixed solution. After the CNT film was sufficiently dried at 80 °C for 10 hours, small discs with diameter of 10 mm (Φ_{10} discs) were cut from it by a laser cutting machine (18W) as the substrate.

Synthesis of Fe-(NiS_2/MoS_2)/CNT film

$Fe(NO_3)_3 \cdot 9H_2O$, $NiCl_2$ and $MoCl_5$ were added into 50ml ethanol in different proportions and stirred for 3 days to get a fully dissolved precursor solution (molar ratios of Ni and Mo were 1: 1, 1: 2 and 1: 3; molar ratios of Fe and Ni were 1:18, 1: 9, 1: 3, 2: 3 and 1: 1, respectively). The CNT film was placed on a heating stage at a temperature of 70 °C, and then the precursor solution was added on it dropwise until the load was about 6 mg. After dried for 1 hour and drilled by laser, the CNT film with micropores was then annealed in a 10% H_2 & 90% Ar atmosphere at 400 °C for 30 minutes. During annealing, a sufficient amount of sulfur powder was placed at the upper end of the airflow and its temperature was maintained at 190 °C. The synthesized Fe-(NiS_2/MoS_2)/CNT film was washed with deionized water and ethanol orderly for 3 minutes and dried before the following electrochemical tests.

Processing of micropores by laser direct writing

This step follows after the precursor loading and before annealing. The laser (λ=1.06 μm) was set to 18 W in power, which drilled through-holes on the film. The obtained micropores on small Φ_{10} discs have a spacing of 800 μm. The average diameter of the pores was about 40 μm, which depends on the size of laser spot and the focusing degree.

Sample characterizations

The morphology of the samples was observed by scanning electron microscope (SEM, ZEISS, Merlin Compact) and transmission electron microscopy (TEM, JEOL, JEM-2010F,200kV). The surface state of the samples was obtained by X-Ray diffraction (XRD, D/max-2500/PC, Rigaku) with Cu Kα radiation (λ= 0.15406 nm) operated at 40 kV and 150 mA. Raman spectra were collected in the range of 200-800 cm^{-1} and X-ray photoelectron spectroscopy (XPS, Thermo Fisher, Escalab 250Xi, Al Kα) in the range of 0 to 1350 eV at a step of 1 eV.

Electrochemical measurements

All electrochemical measures were performed on a CHI 760e electrochemical workstation using a standard three-electrode test. Our samples directly served as the working electrodes. The reference electrode was a saturated calomel electrode (SCE) in acid and neutral solution and Hg/HgO in alkali. A graphite rod was used as a counter electrode. All the potentials were converted to RHE. The polarization curves were measured at 5 mV s^{-1} with 80% iR compensation. The cyclic voltammetry curves for fitting double-layer capacitance (C_{dl}) were measured at 10-50 mV s^{-1} from 0-0.1V vs. RHE. The noble metal electrodes of Pt/C (20 wt%) and RuO_2 were prepared on CNT film with loading of 5mg/cm^{-2} via drop 1 ml of catalyst ink

containing 3.93 mg of catalyst powder, 50 μL of Nafion, 500 μL of ethanol, and 450 μL of distilled water. Electrochemical impedance spectroscopy (EIS) measurements were tested at an overpotential of 300 mV with the frequency range from 10^5 to 10^{-2} Hz with an AC amplitude of 5 mV.

Models of bubbles at the edge of drilled pores and on the surface of electrodes

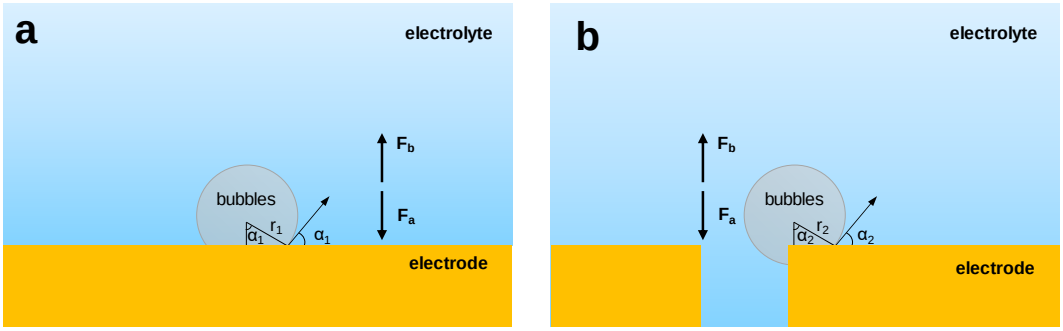

Fig. S1. (a) and (b) show the bubbles on the plane of the electrode and the bubbles at the edge, respectively.

The bubbles maintain the shape of a sphere owing to the intrinsic contact angle of gas and liquid considered to be 180°, Buoyant force (F_b) and adhesion force (F_a)follow the formulas below: [S3]

$$F_b = \rho_{\text{electrolyte}} \cdot g \cdot V_{\text{bubble}} \quad (1)$$

$$F_a = \gamma 2\pi (r \sin\alpha) \sin\alpha \quad (2)$$

Because of the same electrolyte, catalyst, and gas at different sites, the value of contact angles α_1 and α_2 are the same. We assume that there are two bubbles with the same volume attach to the plane and the edge of the electrode, respectively. At this time, $F_{b1} = F_{b2}$ and $r_1 > r_2$ since $V_1 = V_2$.However, F_a is linearly related to radius of bubbles, which result in $F_{a1} > F_{a2}$. So for

the same volume of bubbles, which represents the same number of gas molecules, the F_a on the plane of the electrode is greater than that at the edge, and the bubbles on the plane are more difficult to desorb.

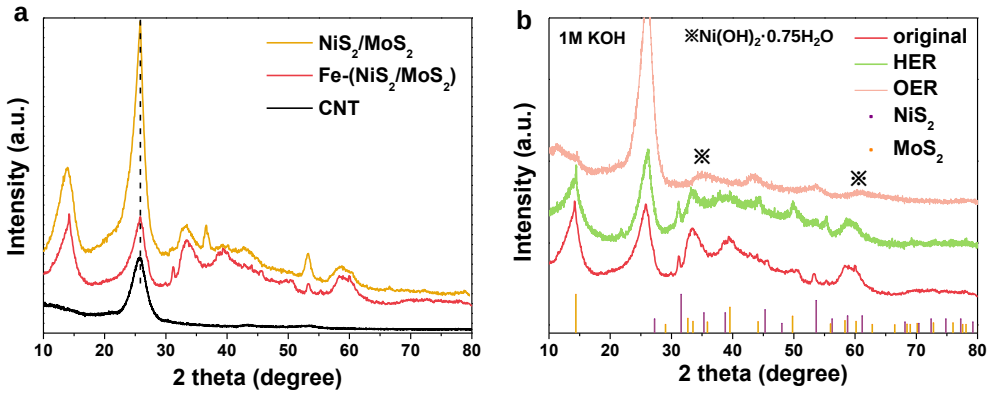

Fig. S2. XRD patterns of (a) Fe-(NiS_2/MoS_2)/CNT, NiS_2/MoS_2/CNT, pure CNT at a range of 10-80 degree, and (b) Comparison between before and after HER and OER stability measures (8h @10 mA cm^{-2}, 8h @100 mA cm^{-2} and 8h @200 mA cm^{-2}).

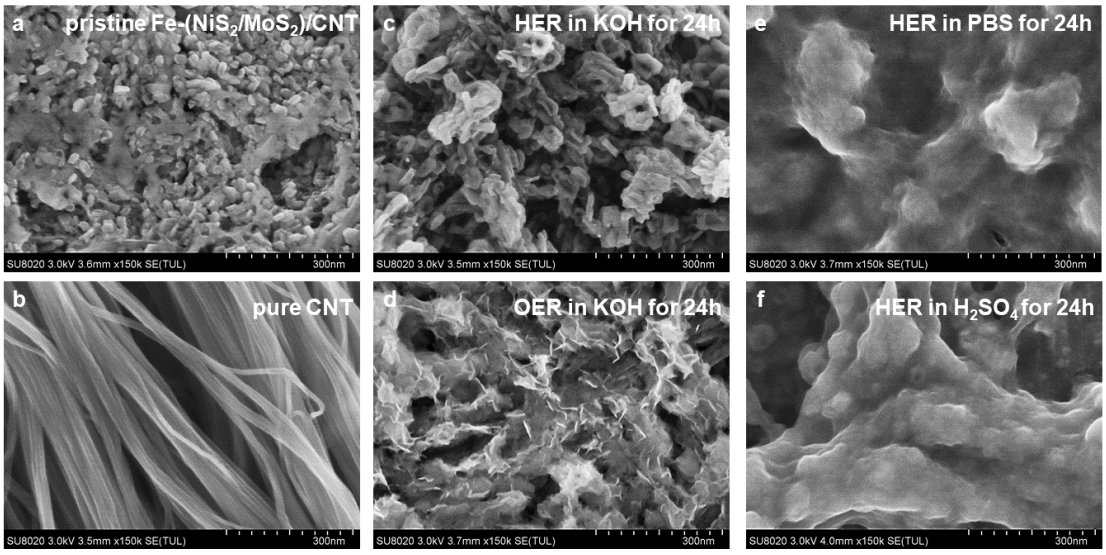

Fig. S3. SEM images of (a) Fe-(NiS_2/MoS_2)/CNT, (b) pure CNT film, (c) Fe-(NiS_2/MoS_2)/CNT after 24h HER in 1M KOH, (d) Fe-(NiS_2/MoS_2)/CNT after 24h OER in 1M KOH, (e) Fe-(NiS_2/MoS_2)/CNT after 24h HER in 1M PBS and (f) Fe-(NiS_2/MoS_2)/CNT after 24h HER in 0.5M H_2SO_4. All the tests were performed at the current density of 10 mA cm^{-2}.

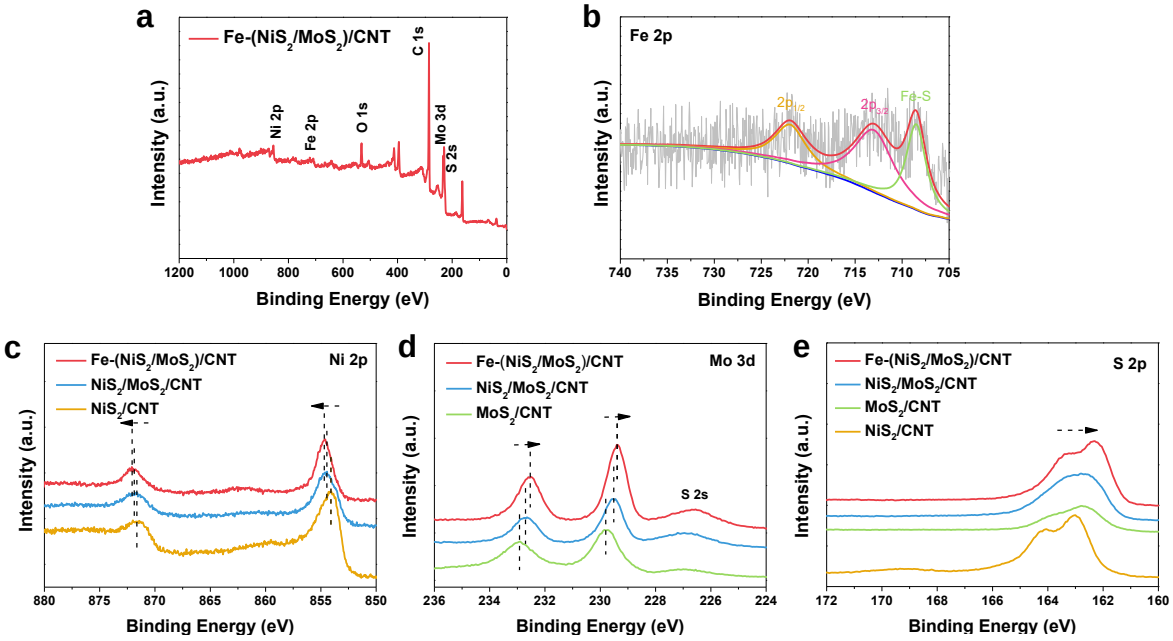

Fig. S4. XPS profiles of (a) Fe-(NiS_2/MoS_2)/CNT survey spectra and (b) Fe 2p of Fe-(NiS_2/MoS_2)/CNT. Comparison of NiS_2/CNT, MoS_2/CNT, NiS_2/MoS_2/CNT and Fe-NiS_2/MoS_2/CNT for (c) Ni 2p, (d) Mo 3d and (e) S 2p.

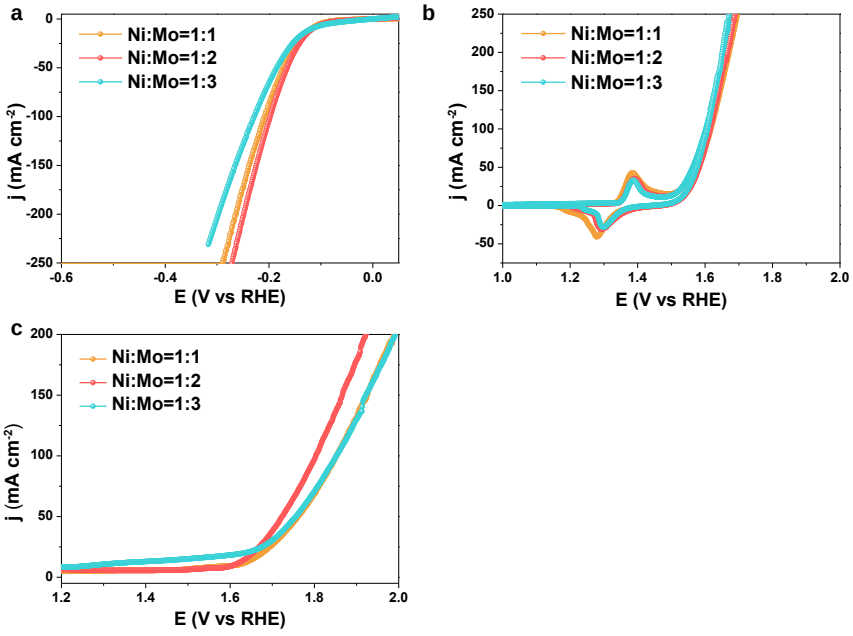

Fig. S5. Polarization curves of electrocatalysts obtained by different ratios of Ni and Mo for NiS_2/MoS_2/CNT in 1M KOH at a scan rate of 5 mV s^{-1} for (a) HER (b) OER and (c) overall water splitting.

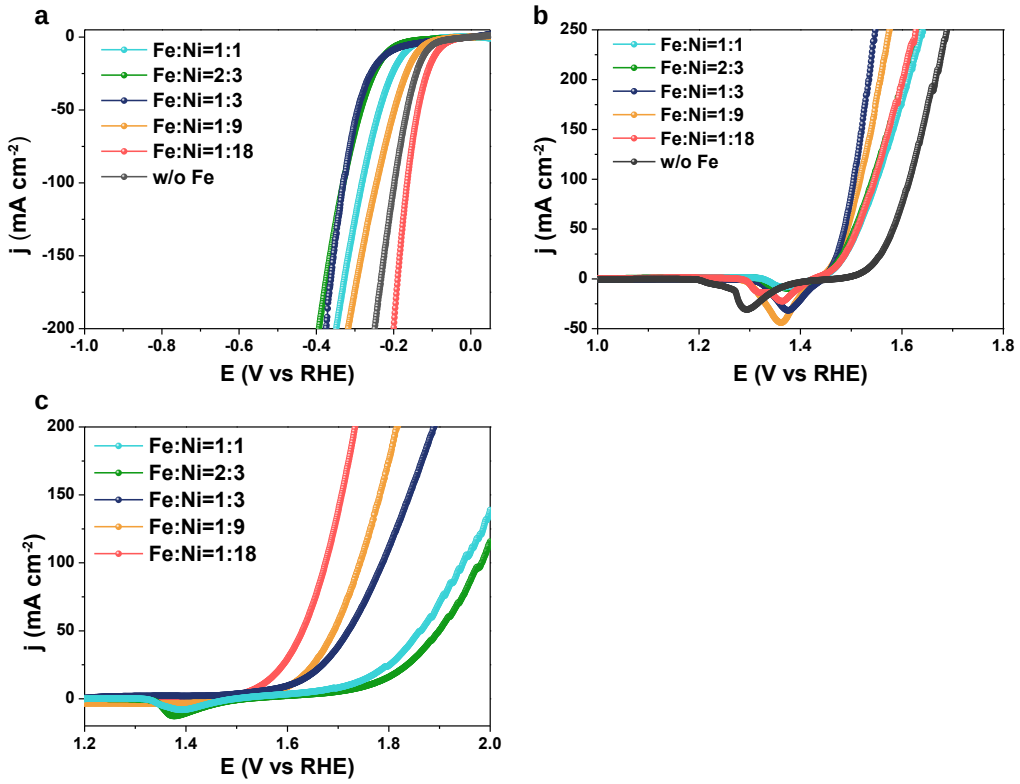

Fig. S6. Polarization curves of electrocatalysts obtained by different ratios of Fe and Ni of Fe-(NiS_2/MoS_2)/CNT in 1M KOH at a scan rate of 5 mV s^{-1} for (a) HER (b) OER and (c) overall water splitting.

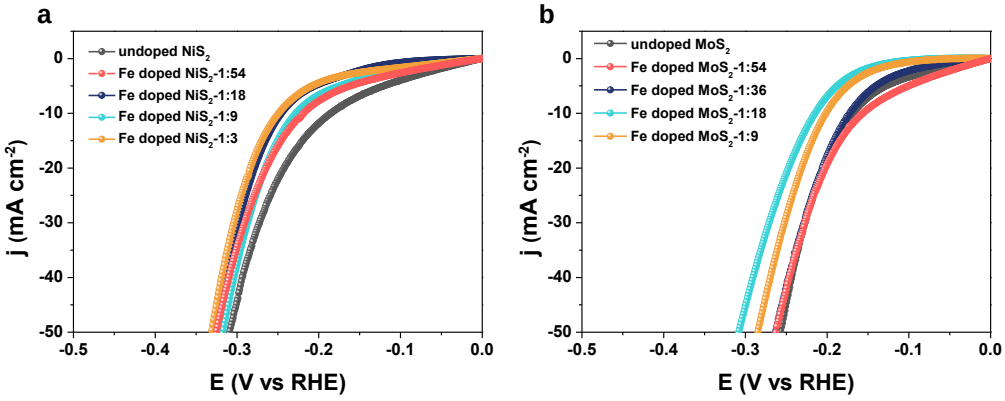

Fig. S7. Polarization curves of (a) NiS_2 and (b) MoS_2 with different Fe doping contents in 1M KOH at a scan rate of 5 mV s^{-1}. The legends in (a) and (b) indicate the Fe:Ni atomic ratio and the Fe:Mo atomic ratio, respectively.

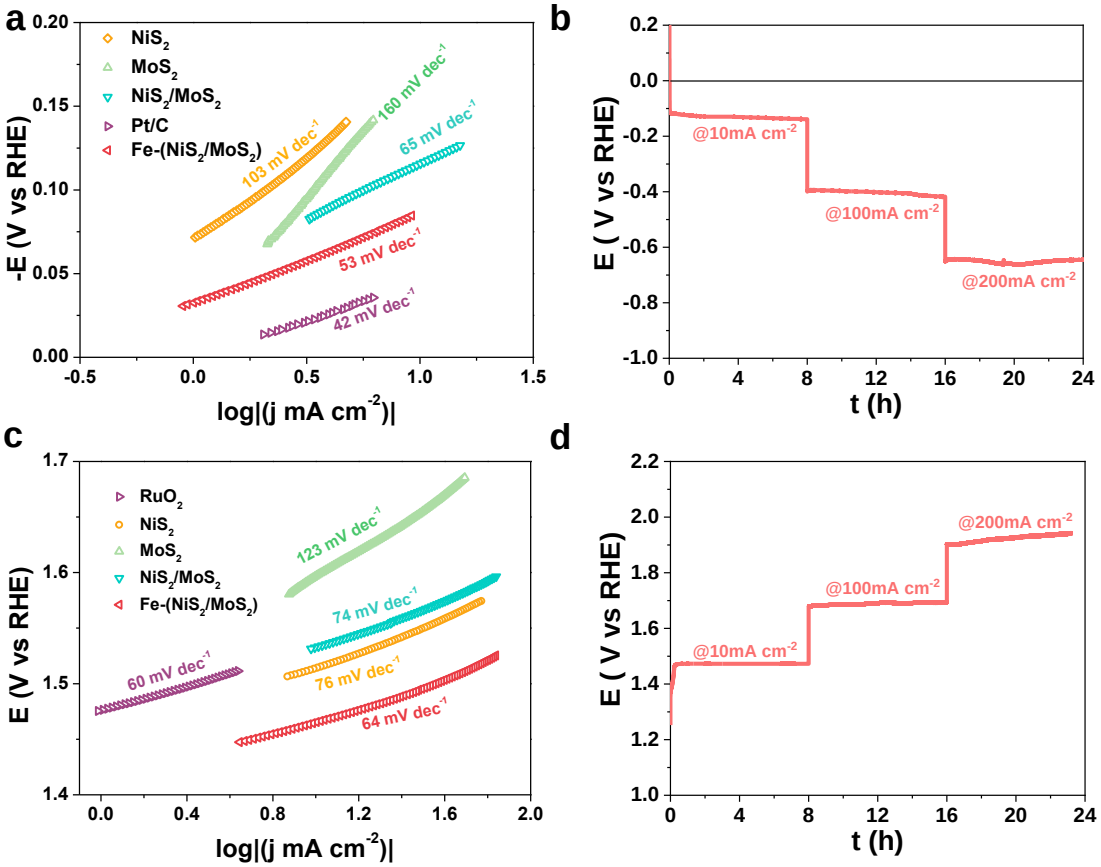

Fig. S8. (a) Tafel plots of various electrocatalysts obtained in 1M KOH at a scan rate of 5 mV s^{-1} for HER. (b) Electrochemical stability test at 10/100/200 mA cm^{-2} of Fe-(NiS_2/MoS_2)/CNT for HER. (c) Tafel plots of various electrocatalysts obtained in 1M KOH at a scan rate of 5 mV s^{-1} for OER. (d) Electrochemical stability test at 10/100/200 mA cm^{-2} of Fe-(NiS_2/MoS_2)/CNT for OER.

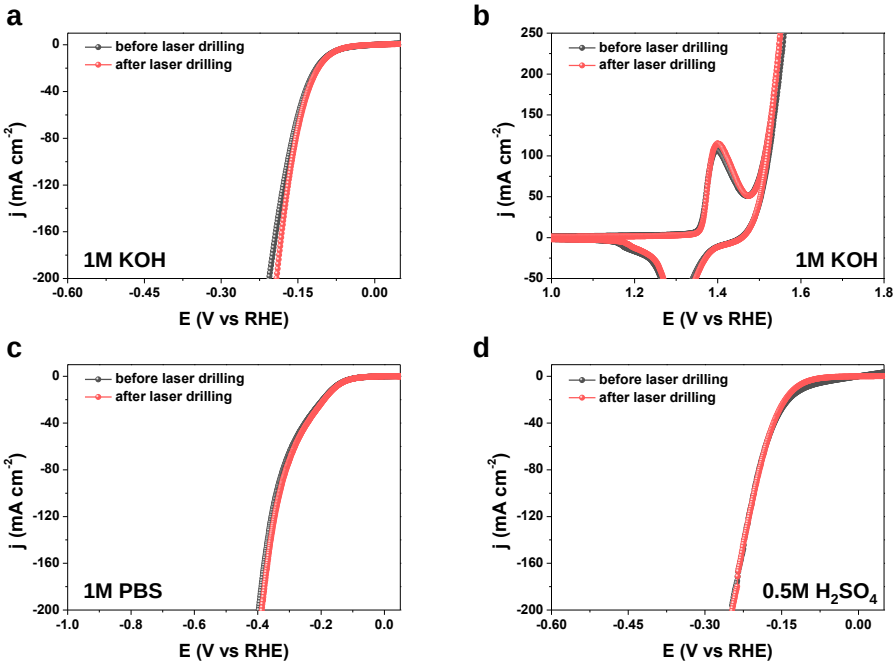

Fig. S9. Electrochemical performance of Fe-(NiS_2/MoS_2)/CNT before and after laser drilling for (a) HER in 1M KOH, (b) OER in 1M KOH, (c) HER in 1M PBS, and (d) HER in 0.5M H_2SO_4. The drilled periodic micropores in the catalyst have a diameter of 40 μm and a spacing of 800 μm.

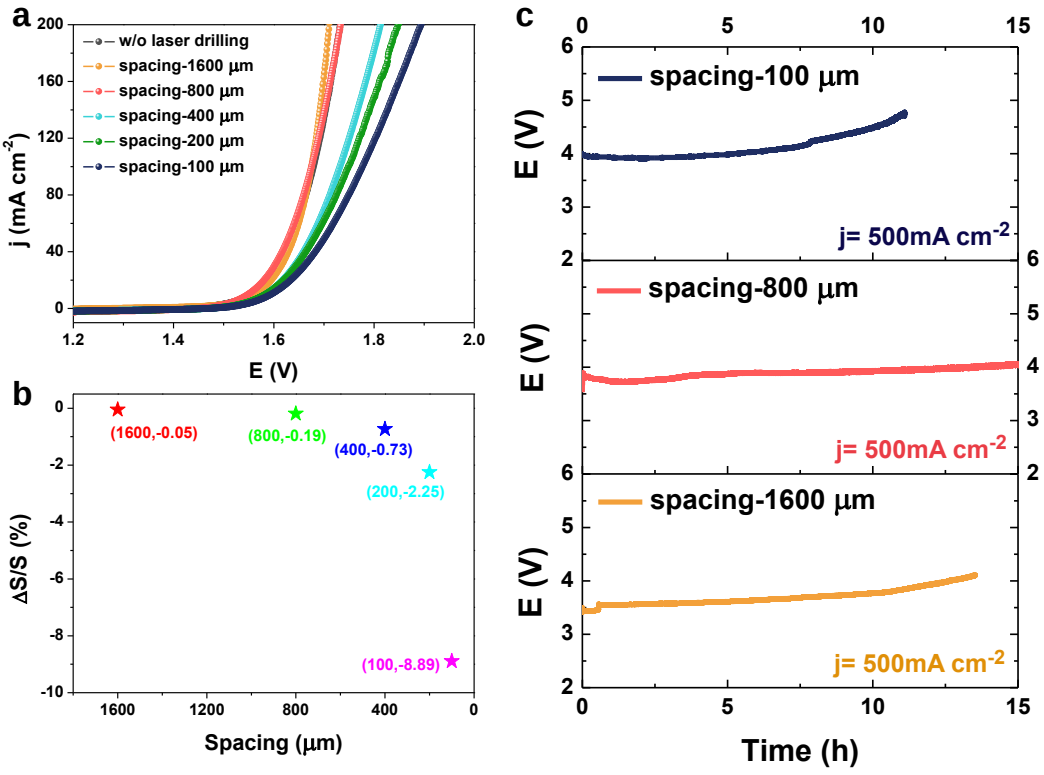

Fig. S10. (a) Polarization curves, (b) estimated surface area loss, and (c) long-term stability

tests at 500 mA cm^{-2} of the Fe-(NiS_2/MoS_2)/CNT electrode drilled with different spacing of micropores.

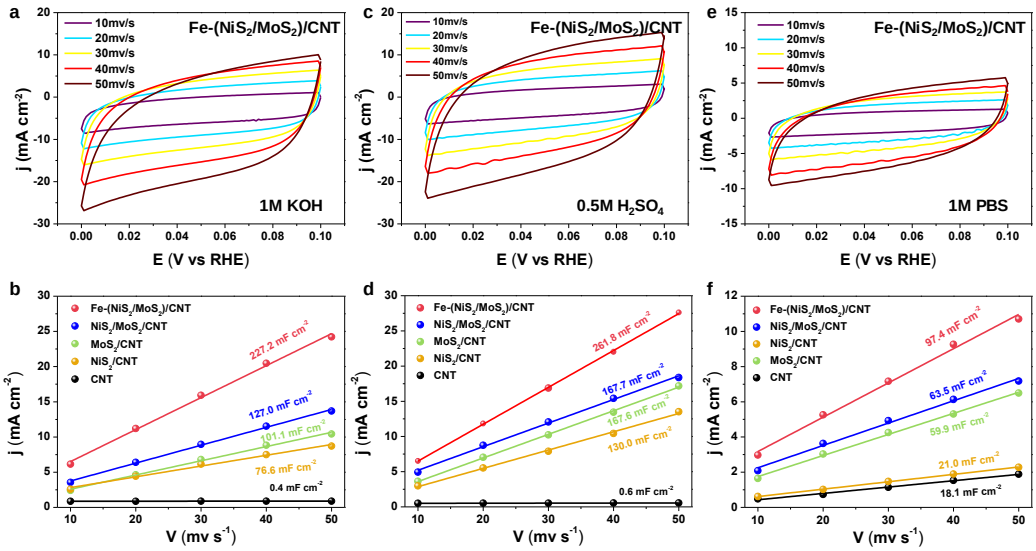

Fig. S11. Cyclic voltammograms (CV) curves of Fe-(NiS_2/MoS_2)/CNT at different scan rates in (a) 1M KOH, (c) 0.5M H_2SO_4, and (e) 1M PBS, and electrochemical C_{dl} of Fe-NiS_2/MoS_2)/CNT, NiS_2/MoS_2/CNT, NiS_2/CNT, MoS_2/CNT, and pure CNT film in (b) 1M KOH, (d) 0.5M H_2SO_4, and (f) 1M PBS.

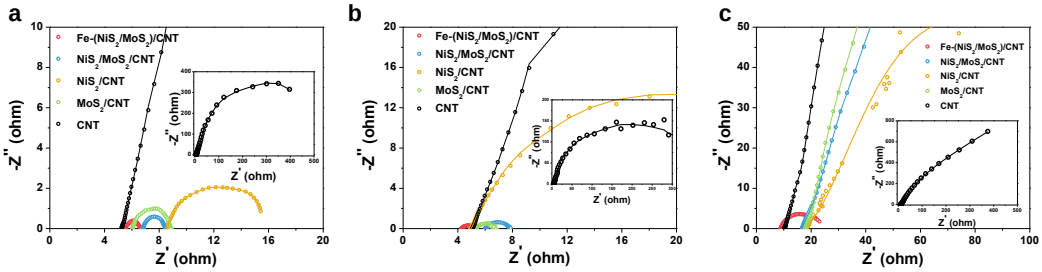

Fig. S12. Nyquist plots of the obtained electrocatalysts at a potential of -300 mV versus RHE in (a) 1M KOH, (b) 0.5M H_2SO_4, and (c) 1M PBS. The AC frequency used in the tests ranges from 10^5 to 10^{-2} Hz with an amplitude of 5 mV.

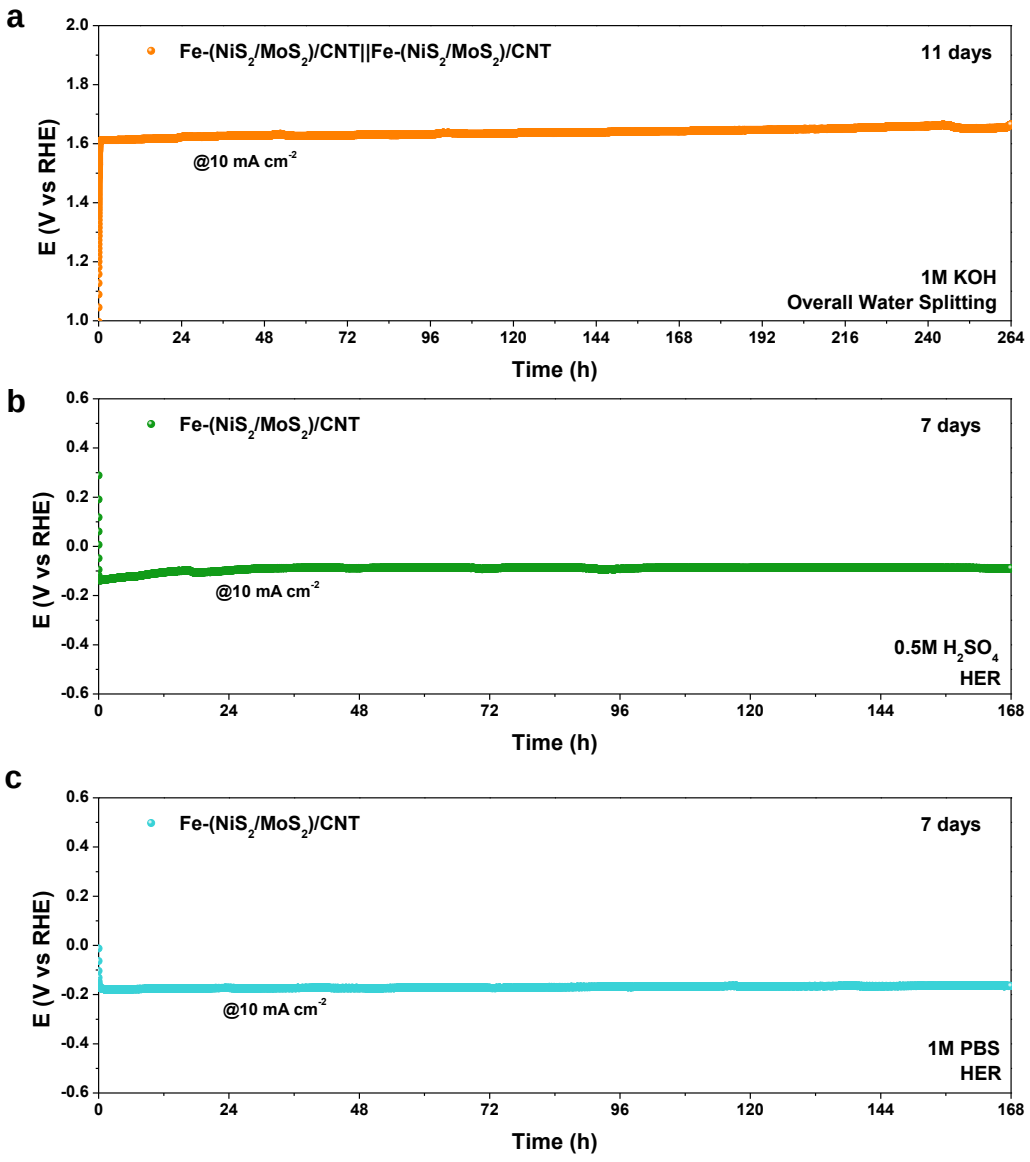

Fig. S13. Long-term test of Fe-(NiS_2/MoS_2)/CNT for (a) overall water splitting in 1M KOH over 11 days, (b) HER in 0.5M H_2SO_4 over 7 days, and (c) HER in 1M PBS over 7 days. All the tests were performed at the current density of 10 mA cm^{-2}.

Table S1. Comparison of our electrode with other overall water splitting catalysts.

catalysts	Voltage @η_{10} (V)	Overpotential of HER @η_{10} (mV)	Overpotential of OER @η_{10} (mV)	Reference
Light Fe-doped (NiS_2/MoS_2)/CNT	**1.51**	**87**	**234**	**This Work**
N-$NiMoO_4$/NiS_2	1.60	57	267	*Adv. Funct. Mater.* 2019,*29,* 1805298.
Ni_3N-VN/NF(HER) Ni_2P-VP_2/NF(OER)	1.51	64	306 @η_{50}	*Adv.Mater.*2019, *31,* 1901174
MoS_2/NiS Yolk–Shell	1.64	244	350	*Small,* 2019, *15,* 1803639.
N-Ni_3S_2/NF	1.48	110	350 @η_{170}	*Adv.Mater.*2017, *29,* 1701584.
V-doped NiS_2	1.56	110	290	*ACS Nano* 2017, *11,* 11574.
$NiFeS_2$/Ni	1.60	126	234 @η_{50}	*J. Mater. Chem. A* 2018, *6,*4346.
MoS_2/NiS_2 Nanosheets	1.59	62	278	*Adv. Sci.* 2019 1900246.
MoS_2/Ni_3S_2	1.56	110	218	*Angew. Chem.* 2016, *128,*6814.
NC/CuCo/$CuCoO_x$	1.53	112	190	*Adv. Funct. Mater.* 2018, *28,* 1704447.
Se-$(NiCo)S_x/(OH)_x$	1.60	103	155	*Adv. Mater.* 2018, *30,* 1705538.
NiFeP/SG	1.54	115	218	*Nano Energy* 2019, *58,* 870.

REFERENCES

(S1) X. Zhang, K. Jiang, C. Feng, P. Liu, L. Zhang, J. Kong, T. Zhang, Q. Li and S. Fan, *Adv. Mater.*, 2006, **18**, 1505-1510.

(S2) K. Liu, Y. Sun, L. Chen, C. Feng, X. Feng, K. Jiang, Y. Zhao and S. Fan, *Nano Lett.*, 2008, **8**, 700-705.

(S3) Z. Lu, Y. Li, X. Lei, J. Liu and X. Sun, *Mater. Horiz.*, 2015, **2**, 294-298.